Int. J. Electron. Commun. (AEÜ) 127 (2020) 153468

Contents lists available at ScienceDirect

International Journal of Electronics and Communications

journal homepage: www.elsevier.com/locate/aeue

Regular paper

On the usage of a time-frequency switch mode algorithm to efficiently simulate RF circuits

Jorge F. Oliveira *

Instituto de Telecomunicações – University of Aveiro, Campus Universitário de Santiago, 3810-193 Aveiro, Portugal
School of Technology and Management – Polytechnic Institute of Leiria, Morro do Lena, Alto Vieiro, Apartado 4163, 2411-901 Leiria, Portugal

ARTICLE INFO

Keywords:
RF circuits
Time–frequency analysis
Circuit simulation

ABSTRACT

Wireless devices integrating more and more features in ever-smaller packages have become integral part of everyone's daily life. These systems have seen a continuous push to profit from digital signal processing techniques, in which signals are no longer traditional continuous amplitude and/or phase-modulated carriers, but became pulsed waveforms where the amplitude and/or phase are coded in some on–off digital scheme. This on–off scenario has been addressing new challenges to the circuit-level simulation of such systems. Having this in mind this paper aims to propose an innovative time–frequency simulation technique based on a switch mode algorithm, which is specially conceived for the efficient numerical simulation of RF circuits whose stimuli are intermittently turned on and off for unknown periods of time. At present, to simulate this category of circuits commercial tools have no choice than to make use of full conventional SPICE algorithms. This paper suggests an alternative way, which can result in significant speedups, without perceptible loss in accuracy.

1. Introduction

A significant advancement has been made in electronic circuit-level simulation in the last years. This is particularly true in the RF and microwave areas, where several innovative CAD techniques have been successively published in the scientific literature. Numerical simulation techniques based on state variables and waves [1], advanced techniques based on multivariate formulations [2], innovative techniques based on multi-rate approaches [3–5], improved versions of conventional time-domain [6,7] and frequency domain [8–10] techniques, innovative algorithms based on wise circuit subset partition [11,12], and wavelet based methods [13], are illustrative examples of the research work conducted in this area. Despite the achievements brought by these techniques there are still some outstanding challenges in the RF CAD research field. A clear example of that is the simulation of circuits whose stimuli are randomly turned on and off for unknown periods of time. RF circuits subject to on–off digital modulation (e.g., on–off keying (OOK) transceivers used in low-power or ultra low-power applications [14–17], amplitude-burst wireless transmitters [18], or pulsed load modulators conceived for efficient power amplification [19,20]), are illustrative application examples where this situation occurs. Because the circuits are left to their natural response states when the forcing functions are switched off (unforced or autonomous behavior), only traditional time-step integration schemes, as Runge-Kutta (RK) methods or linear multistep methods (LMM), are suitable to simulate this kind of circuits. Unfortunately, time-step integration engines are, in general, very inefficient when applied to RF systems, requiring a large amount of memory and computational time. To cope with this challenging scenario, of the stimuli being continuously turned on and off for unknown periods of time, an innovative simulation technique based on a time-slot partitioning approach was already proposed in [12]. However, the approach adopted in [12] has conducted to a purely time-domain technique, in which the simulation algorithm is automatically switched between an envelope transient over shooting engine and a time-step integration scheme, according to the presence, or absence, of stimulus, respectively. The main weakness of the simulation technique proposed in [12] is that it is not able to take advantage of the circuits' moderate nonlinearities, and their corresponding smooth narrowband RF modulated signals, which can be more efficiently computed in the frequency domain. To circumvent this limitation this work proposes a switch mode algorithm, which combines a hybrid time–frequency scheme with a pure time-step integration engine. The hybrid scheme will be used for the time slots in which the circuits' stimuli are turned on, whereas the time-step integration scheme will be used for the time slots in which the stimuli are

* At: School of Technology and Management – Polytechnic of Leiria, Morro do Lena, Alto Vieiro, Apartado 4163, 2411-901 Leiria, Portugal.
E-mail address: jorge.oliveira@ipleiria.pt.

https://doi.org/10.1016/j.aeue.2020.153468
Received 29 May 2020; Accepted 16 September 2020
Available online 21 September 2020

switched off, i.e., whenever the circuits are left to their natural response states.

Contrary to previously published techniques [4,5] that also combined hybrid schemes with time-step integration engines, the method presented in this paper does not rely on any circuit block division strategy, but, instead, on a time-slot partitioning stratagem. Moreover, it must be pointed out that the switch mode simulation algorithm proposed in this paper is quite distinct from any other time–frequency technique previously published in the scientific literature (or used by commercial tools). In fact, the basic assumption of hybrid time–frequency techniques, as ETHB, or multitime ETHB [21,22], or other well established envelope following techniques, becomes their main drawback. By requiring the circuits to be excited by stimuli containing a periodic component (e.g., an RF carrier), these simulation tools are not appropriate to deal with circuits excited by aperiodic forcing functions, or circuits left in their natural response states when forcing functions are switched off. This work proposes an innovative numerical simulation technique to overcome this difficulty.

In order to provide a general overview on the now proposed simulation technique, this paper is organized as follows. After this short introduction, Section 2 provides some general background material on circuit simulation, as well as a brief review of the numerical techniques on which the structure of the now proposed method is inspired. Section 3 is devoted to the presentation of the most important details of the method, such as the time slot partitioning strategy, the adopted numerical schemes and the transition between them. Section 4 describes the application of the method to two illustrative application examples, and finally, Section 5 summarizes the most important conclusions of this work.

2. Review of theoretical background

2.1. General DAE formulation

Systems of nonlinear differential algebraic equations (DAE) are an appropriate representation widely used for modelling the dynamic behaviour of electronic circuits. These systems, involving voltages, currents, charges and fluxes, are usually obtained via nodal analysis, or modified nodal analysis (MNA), which consists in applying the Kirchhoff currents' law (KCL) to each electrical node and writing the branch currents in terms of the circuit node voltages using the corresponding constitutive relations to each circuit element. Such systems have, in general, the following form,

$$\boldsymbol{p}(\boldsymbol{y}(t)\,) + \frac{d\boldsymbol{q}(\boldsymbol{y}(t)\,)}{dt} = \boldsymbol{x}(t), \tag{2.1}$$

in which $\boldsymbol{x}(t) \in \mathbb{R}^N$ is the vector of independent stimuli (voltage or current sources) to the circuit, $\boldsymbol{y}(t) \in \mathbb{R}^N$ is the vector of unknowns (voltages and currents waveforms) and N is the total number of unknowns. $\boldsymbol{p} : \mathbb{R}^N \rightarrow \mathbb{R}^N$ describes the memoryless elements in the circuit (linear and nonlinear elements, as resistors, nonlinear voltage-controlled current sources, etc.), while $\boldsymbol{q} : \mathbb{R}^N \rightarrow \mathbb{R}^N$ models all linear and nonlinear reactive circuit elements, as capacitors or inductors, represented as voltage-dependent electric charges, or current-dependent magnetic fluxes, respectively.

2.2. Univariate time-step integration (SPICE-like simulation)

The most natural way of simulating the dynamic behavior of an electronic circuit is to numerically time-step integrate, in time domain, the DAE system modeling its operation. This straightforward technique was used in the first digital computer programs of circuit analysis and is still nowadays the most widely used numerical method for that purpose. It is present in all SPICE (which means Simulation Program with Integrated Circuit Emphasis) or SPICE-like computer programs. With this technique the solution of (2.1) is computed over a specified time interval $[t_0, t_{Final}]$ from a specific initial condition $\boldsymbol{y}(t_0) = \boldsymbol{y}_0$.

In order to numerically time-step integrate (2.1), one can use initial value solvers, such as standard Runge-Kutta (RK) methods [23,24], or linear multistep methods (LMM) [23,24]. Both of these classes of methods can provide a wide variety of explicit and implicit numerical schemes, with very distinct properties in terms of order (accuracy) and numerical stability. Most SPICE implementations are based on second order LMM methods, as Gear-2, trapezoidal or modified trapezoidal schemes.

2.3. Multivariate formulation

The multivariate formulation is a useful stratagem that plays an important role in the electronic design automation (EDA) community, especially in the RF and microwave areas. It was initially introduced in 1996 [25] and it has been adopted by diverse researchers, which have demonstrated that it can be an efficient strategy when dealing with electronic circuits operating on widely distinct time scales. The success of multivariate formulation relies on the fact that voltages and currents containing components that evolve themselves at two, or more, widely separated rates of variation can be represented much more efficiently if we define them as functions of two, or more, time variables (artificial time scales). With this stratagem all signals (stimuli and responses) will be represented as multivariate functions, which will imply that dynamic behavior of the circuits will not be modeled by DAE systems formulated in the one dimensional time, but instead, by partial differential systems.

The following procedure can be adopted for both vector-valued functions $\boldsymbol{x}(t)$ and $\boldsymbol{y}(t)$ in the DAE system of (2.1): t is replaced by t_1 in the slowly varying entities and t is replaced by t_2 in the fast-varying entities. The application of this stratagem will turn (2.1) into the following multitime partial differential algebraic equations' (MPDAE) system

$$\boldsymbol{p}(\widehat{\boldsymbol{y}}(t_1,t_2)\,) + \frac{\partial \boldsymbol{q}(\widehat{\boldsymbol{y}}(t_1,t_2)\,)}{\partial t_1} + \frac{\partial \boldsymbol{q}(\widehat{\boldsymbol{y}}(t_1,t_2)\,)}{\partial t_2} = \widehat{\boldsymbol{x}}(t_1,t_2), \tag{2.2}$$

where $\widehat{\boldsymbol{x}}(t_1,t_2) \in \mathbb{R}^N$ and $\widehat{\boldsymbol{y}}(t_1,t_2) \in \mathbb{R}^N$ are the bivariate forms of $\boldsymbol{x}(t)$ and $\boldsymbol{y}(t)$, respectively. It is straightforward to demonstrate that, if $\widehat{\boldsymbol{x}}(t_1,t_2)$ and $\widehat{\boldsymbol{y}}(t_1,t_2)$ satisfy (2.2), then the univariate forms $\boldsymbol{x}(t) = \widehat{\boldsymbol{x}}(t,t)$ and $\boldsymbol{y}(t) = \widehat{\boldsymbol{y}}(t,t)$ satisfy (2.1) [26]. Thus, taking into account the periodicity of the problem in the t_2 fast artificial time scale, the one dimensional version of the vector containing the circuit responses is acquired from its bivariate representation as

$$\boldsymbol{y}(t) = \widehat{\boldsymbol{y}}(t, t \bmod T_2), \tag{2.3}$$

where $t \bmod T_2$ represents the remainder of division of t by T_2.

2.4. Envelope modulated regimes

Envelope modulated regimes are typical cases of practical interest and correspond to a combination of initial and periodic boundary conditions for the MPDAE of (2.2) [2]. This means that the bivariate forms of these solutions can be obtained by numerically solving the following initial-boundary value problem

$$\boldsymbol{p}(\widehat{\boldsymbol{y}}(t_1,t_2))+\frac{\partial \boldsymbol{q}(\widehat{\boldsymbol{y}}(t_1,t_2))}{\partial t_1}+\frac{\partial \boldsymbol{q}(\widehat{\boldsymbol{y}}(t_1,t_2))}{\partial t_2}=\widehat{\boldsymbol{x}}(t_1,t_2)\widehat{\boldsymbol{y}}(0,t_2)=\boldsymbol{\psi}(t_2),\quad \widehat{\boldsymbol{y}}(t_1,0)=\widehat{\boldsymbol{y}}(t_1,T_2) \tag{2.4}$$

on the rectangle $[0,t_{Final}]\times[0,T_2]$, in which $[0,t_{Final}]$ is the simulation interval and T_2 is the carrier period. $\boldsymbol{\psi}(\cdot)\in\mathbb{R}^N$ is a given initial-condition function defined on $[0,T_2]$, satisfying $\boldsymbol{\psi}(0)=\boldsymbol{\psi}(T_2)=\boldsymbol{y}(0)$, and the periodic boundary condition $\widehat{\boldsymbol{y}}(t_1,0)=\widehat{\boldsymbol{y}}(t_1,T_2)$ is due to the periodicity of the problem in the t_2 fast carrier time scale. The reason why bivariate envelope modulated solutions do not need to be evaluated on the entire $[0,t_{Final}]\times[0,t_{Final}]$ domain, and are restricted to the rectangle $[0,t_{Final}]\times[0,T_2]$, is because the solutions repeat along the t_2 time axis. The way how univariate solutions are recovered from their multivariate forms was already defined above by (2.3).

Consider the semi-discretization of the rectangular domain $[0,t_{Final}]\times[0,T_2]$ in the t_1 slow time dimension defined by some grid

$$0=t_{1,0}<t_{1,1}<\cdots<t_{1,i-1}<t_{1,i}<\cdots<t_{1,K_1}=t_{Final},\qquad h_{1,i}=t_{1,i}-t_{1,i-1}, \tag{2.5}$$

where K_1 represents the total number of steps in t_1. Then, replace the partial derivatives of (2.4) in t_1 with a finite-differences approximation. Taking into account the periodicity of the problem in the t_2 fast time scale, i.e., $\widehat{\boldsymbol{y}}(t_{1,i},0)=\widehat{\boldsymbol{y}}(t_{1,i},T_2)$, a boundary value problem with periodic boundary conditions is obtained for each slow time instant $t_{1,i}$, from $i=1$ to $i=K_1$. For instance, if the BDF2 [23] backward-differentiation-formula is used to approximate the derivatives of (2.4) in t_1, one obtains

There are several numerical techniques that can be used to solve (2.6). However, when waveforms are not extremely demanding on the number of harmonics for a convenient frequency-domain representation, a particular technique has been found particularly useful: the harmonic balance (HB) method [27,28].

3. Innovative switch mode simulation technique

3.1. Basic slot partitioning strategy

Changing the algorithm throughout the evaluation of the numerical solution of a DAE system, or ODE system, is an idea that is far from being new. For instance, some initial value solvers available on commercial tools use cheap explicit schemes for time slots in which differential systems are not stiff and utilize robust implicit schemes for intervals in which stiffness is detected. Another example involving a time-slot partitioning strategy regarding different algorithms for different time intervals (time slots) [12] was already mentioned in the introduction of this paper.

The main novelty behind the technique proposed in this paper relies on the fact that there are time slots in which the numerical algorithm

$$\boldsymbol{p}(\widehat{\boldsymbol{y}}_i(t_2))+3\boldsymbol{q}(\widehat{\boldsymbol{y}}_i(t_2))-4\boldsymbol{q}\left(\frac{\widehat{\boldsymbol{y}}_{i-1}(t_2))+\boldsymbol{q}(\widehat{\boldsymbol{y}}_{i-2}(t_2))}{2h_{1,i}}+\frac{d\boldsymbol{q}(\widehat{\boldsymbol{y}}_i(t_2))}{dt_2}=\widehat{\boldsymbol{x}}\left(t_{1,i},t_2\right),\widehat{\boldsymbol{y}}_i(0)=\widehat{\boldsymbol{y}}_i(T_2). \tag{2.6}$$

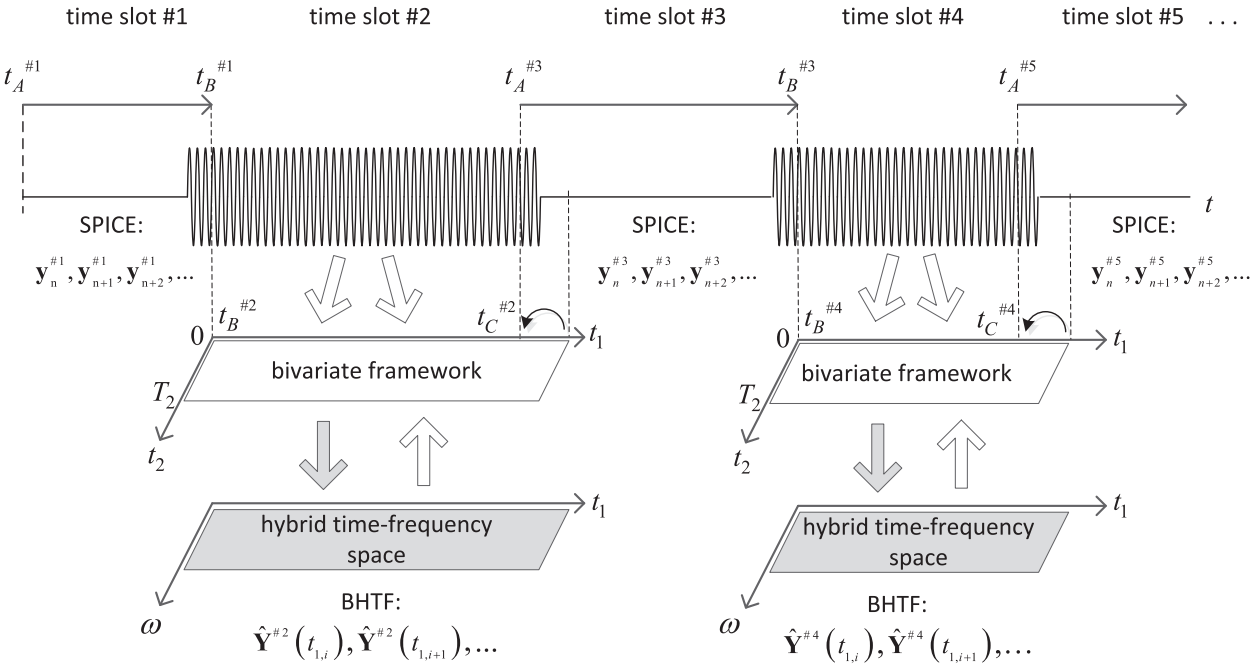

Fig. 3.1. Time-slot partitioning technique for switching between the transient response computed with SPICE and the forced response calculated with the BHTF scheme.

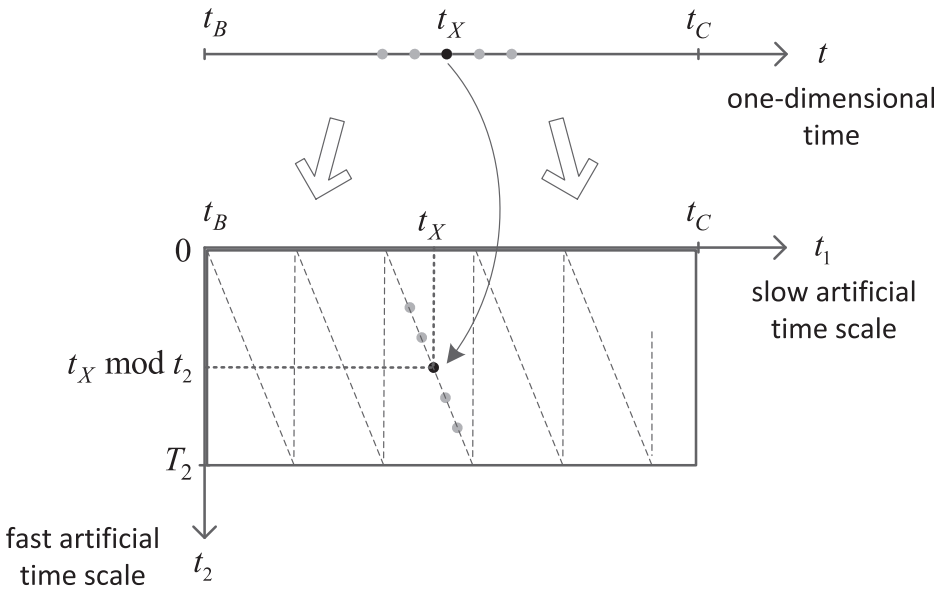

Fig. 3.2. Decoupling univariate time into two artificial time scales. The sawtooth path is defined by (2.3).

operates strictly in the one dimensional time, whereas in other time slots it works in a multivariate hybrid time–frequency framework. For achieving an intuitive explanation of method, let us consider a circuit whose stimulus (e.g. a carrier signal) is randomly turned on and off, like the signal depicted in Fig. 3.1. The proposed method will simulate the circuit using (i) a purely time-domain time-step integration engine (here abbreviated as SPICE) and (ii) a bivariate hybrid time–frequency scheme (here abbreviated as BHTF). The SPICE engine will be mainly used for the time slots where there is no stimulus, and so the circuit exhibits a transient response due to the RF energy stored in its reactive components. The BHTF scheme will be used for some specific portions of the time slots where the stimulus is turned on, and so the circuit responds with a forced response due to a periodic RF carrier (eventually modulated by some slowly varying envelope).

3.2. Numerical schemes

3.2.1. Univariate time-domain schemes

When there is no stimulus, i.e., during the intervals in which the circuit is not forced by any independent source, the solution of the circuit has to be computed with a SPICE engine. Indeed, only conventional time-step integration schemes are suitable to simulate the dynamic behavior of the circuit under such circumstances. Hence, we have no other way than to use initial value solvers, such as linear multistep methods (LMM) or Runge-Kutta (RK) schemes. Since most popular SPICE implementations available on both commercial and free simulation packages are based on Gear-2, trapezoidal or modified trapezoidal schemes [23], separated simulation tests considering each one of these three methods as the preferred SPICE algorithm were firstly conducted for computing the numerical solution in the intervals in which the circuit is not forced by any independent source. Additionally, conventional Runge-Kutta (RK) and multirate Runge-Kutta (MRK) schemes were also used for this purpose.

$\boldsymbol{y}_n \simeq \boldsymbol{y}(t_n)$, $\boldsymbol{y}_{n+1} \simeq \boldsymbol{y}(t_{n+1})$, $\boldsymbol{y}_{n+2} \simeq \boldsymbol{y}(t_{n+2})$, …, denote the numerical solution at the time instants t_n, t_{n+1}, t_{n+2}, …, respectively, using a time-step integration size defined as $h = t_{n+1} - t_n = t_{n+2} - t_{n+1} = \cdots$. Thus, the numerical solution of the circuit in some specific time window $[t_A, t_B]$ is obtained step by step, starting from $t = t_A$, with a specific initial condition, $\boldsymbol{y}(t_A) \in \mathbb{R}^N$, previously given by the scheme adopted in the previous time window, until $t = t_B$.

The use of several different versions for the univariate time-domain scheme (Gear-2, trapezoidal, modified trapezoidal, RK and MRK) was here adopted with the purpose of attesting the potential influence of the chosen SPICE algorithm in the global performance of the new proposed simulation technique. As will be seen in the experiments reported in Section 4, the effectiveness of the new proposed technique is practically independent of the SPICE implementation considered for the time slots in which there is no stimulus.

3.2.2. Bivariate hybrid time–frequency (BHTF) scheme

Let us now focus on the time intervals in which the circuit is forced by an independent source containing a periodic component (e.g., an envelope modulated signal, or simply an RF carrier). When the stimulus is turned on we are able to use the hybrid scheme to compute the solution of the circuit. This means that if we want to evaluate the numerical solution of the circuit in some specific $[t_B, t_C]$ time window, at first we have to map the one-dimensional interval $[t_B, t_C]$ into the $[t_B, t_C] \times [0, T_2]$ rectangular region defined in the t_1, t_2 bidimensional space. This is illustrated in Figs. 3.1 and 3.2.

Then, the $[t_B, t_C] \times [0, T_2]$ rectangular region is discretized in both the t_1 and t_2 dimensions according to the following grid

$$\begin{aligned} &t_B = t_{1,0} < t_{1,1} < \cdots < t_{1,i-1} < t_{1,i} < \cdots < t_{1,K_1} = t_C, \quad h_{1,i} = t_{1,i} - t_{1,i-1}, \\ &0 = t_{2,0} < t_{2,1} < \cdots < t_{2,j-1} < t_{2,j} < \cdots < t_{2,K_2} = T_2, \quad h_2 = t_{2,j} - t_{2,j-1} = T_2/K_2, \end{aligned} \tag{3.1}$$

which can be nonuniform in t_1 and which contains a total of $(K_1 + 1) \times (K_2 + 1)$ grid points. However, since HB represents the circuit fast variations $\widehat{y}(t_{1,i}, t_2)$ as a collection of Fourier coefficients, and not a as a collection of time samples, the t_2 fast artificial time scale will be converted into the frequency domain, in which a convenient harmonic truncation at some order K is adopted. Hence, $K_2 \geqslant 2K + 1$.

The system of (2.6) is firstly converted into the following slow time varying HB system

$$\boldsymbol{P}\left(\widehat{\boldsymbol{Y}}\left(t_{1,i},k\omega_p\right)\right)+3\boldsymbol{Q}\left(\widehat{\boldsymbol{Y}}\left(t_{1,i},k\omega_p\right)\right)-4\boldsymbol{Q}\left(\frac{\widehat{\boldsymbol{Y}}\left(t_{1,i-1},k\omega_p\right)+\boldsymbol{Q}\left(\widehat{\boldsymbol{Y}}\left(t_{1,i-2},k\omega_p\right)\right)}{2h_{1,i}}+j\boldsymbol{\Omega}\boldsymbol{Q}\left(\widehat{\boldsymbol{Y}}\left(t_{1,i},k\omega_p\right)\right)=\widehat{\boldsymbol{X}}\left(t_{1,i},k\omega_p\right), \tag{3.2}$$

where $\widehat{\boldsymbol{X}}\left(t_{1,i},k\omega_p\right)\in\mathbb{C}^{N\times(2K+1)}$ and $\widehat{\boldsymbol{Y}}\left(t_{1,i},k\omega_p\right)\in\mathbb{C}^{N\times(2K+1)}$ are the vectors containing the Fourier coefficients of the excitation and the solution for all $v=1,2,\ldots,N$ unknowns (the circuit state variables), respectively, at each slow time instant $t_1=t_{1,i}$. $\boldsymbol{P}(\cdot):\mathbb{C}^{N\times(2K+1)}\to\mathbb{C}^{N\times(2K+1)}$ and $\boldsymbol{Q}(\cdot):\mathbb{C}^{N\times(2K+1)}\to\mathbb{C}^{N\times(2K+1)}$ are nonlinear complex functions that can be computed by evaluating p(.) and q(.) in time domain and then calculating their Fourier coefficients. $\boldsymbol{\Omega}$ is a $N\times(2K+1)$ diagonal matrix defined as

$$\boldsymbol{\Omega}=\begin{pmatrix}\Omega_1 & & 0\\ & \ddots & \\ 0 & & \Omega_N\end{pmatrix},\quad \Omega_1=\cdots=\Omega_N=\mathrm{diag}\left(-K\omega_p,\ldots,K\omega_p\right), \tag{3.3}$$

where K is the order of the adopted harmonic truncation and $\omega_p=2\pi f_C$ is the carrier frequency.

The objective is to compute $\widehat{\boldsymbol{Y}}\left(t_{1,i},k\omega_p\right)\in\mathbb{C}^{N\times(2K+1)}$, i.e., the vectors containing the Fourier coefficients of the solution, for all $v=1,2,\ldots,N$ unknowns, from $t_{1,i}=t_{1,1}$ to $t_{1,i}=t_{1,K_1}=t_C$, starting from a previously given initial condition $\widehat{\boldsymbol{Y}}\left(t_{1,0},k\omega_p\right)\in\mathbb{C}^{N\times(2K+1)}$. For that, the system of (3.2) is iteratively solved according to the following rule

$$j\boldsymbol{\Omega}\boldsymbol{Q}\left(\widehat{\boldsymbol{Y}}^{[r]}\left(t_{1,i},k\omega_p\right)\right)+3\boldsymbol{Q}\left(\widehat{\boldsymbol{Y}}^{[r]}\left(t_{1,i},k\omega_p\right)\right)-4\boldsymbol{Q}\left(\frac{\widehat{\boldsymbol{Y}}\left(t_{1,i-1},k\omega_p\right)+\boldsymbol{Q}\left(\widehat{\boldsymbol{Y}}\left(t_{1,i-2},k\omega_p\right)\right)}{2h_{1,i}}+\boldsymbol{P}\left(\widehat{\boldsymbol{Y}}^{[r]}\left(t_{1,i},k\omega_p\right)\right)-\widehat{\boldsymbol{X}}\left(t_{1,i},k\omega_p\right)+\left[j\boldsymbol{\Omega}\boldsymbol{C}\left(\widehat{\boldsymbol{Y}}^{[r]}\left(t_{1,i},k\omega_p\right)\right)\right.$$
$$\left.+\frac{3}{2h_{1,i}}\boldsymbol{C}\left(\widehat{\boldsymbol{Y}}^{[r]}\left(t_{1,i},k\omega_p\right)\right)+\boldsymbol{G}\left(\widehat{\boldsymbol{Y}}^{[r]}\left(t_{1,i},k\omega_p\right)\right)\right]\times\left[\widehat{\boldsymbol{Y}}^{[r+1]}\left(t_{1,i},k\omega_p\right)-\widehat{\boldsymbol{Y}}^{[r]}\left(t_{1,i},k\omega_p\right)\right]=0, \tag{3.4}$$

which means that at each iteration r a linear system of $N\times(2K+1)$ complex equations have to be solved to compute the new estimate $\widehat{\boldsymbol{Y}}^{[r+1]}\left(t_{1,i},k\omega_p\right)$ from the previous one. Consecutive iterations will be conducted until the desired accuracy criteria are satisfied. For large size circuits GMRES is the preferred method to solve (3.4).

The time varying Jacobian matrix in (3.4) is a block matrix formed from N^2 sets of $(2K+1)\times(2K+1)$ time varying submatrices. As can be seen, each submatrix is evaluated as a combination of $\boldsymbol{C}\left(\widehat{\boldsymbol{Y}}\left(t_{1,i},k\omega_p\right)\right)$ and $\boldsymbol{G}\left(\widehat{\boldsymbol{Y}}\left(t_{1,i},k\omega_p\right)\right)$, which are themselves computed as follows. For the general block of row m and column l $\boldsymbol{C}_{ml}\left(\widehat{\boldsymbol{Y}}\left(t_{1,i},k\omega_p\right)\right)$ and $\boldsymbol{G}_{ml}\left(\widehat{\boldsymbol{Y}}\left(t_{1,i},k\omega_p\right)\right)$ are given as

$$\boldsymbol{C}_{ml}\left(\widehat{\boldsymbol{Y}}\left(t_{1,i},k\omega_p\right)\right)=\mathrm{Toeplitz}\left\{\mathrm{DFT}\left[c_{ml}\left(t_{1,i},t_2\right)=\frac{dq_m\left(\widehat{y}\left(t_{1,i},t_2\right)\right)}{d\widehat{y}_l\left(t_{1,i},t_2\right)}\right]\right\}, \tag{3.5}$$

and

$$\boldsymbol{G}_{ml}\left(\widehat{\boldsymbol{Y}}\left(t_{1,i},k\omega_p\right)\right)=\mathrm{Toeplitz}\left\{\mathrm{DFT}\left[g_{ml}\left(t_{1,i},t_2\right)=\frac{dp_m\left(\widehat{y}\left(t_{1,i},t_2\right)\right)}{d\widehat{y}_l\left(t_{1,i},t_2\right)}\right]\right\}, \tag{3.6}$$

i.e., as the Toeplitz matrices of vectors containing the slow time varying Fourier coefficients (truncated at some order $k=K$) of the nonlinear functions $c_{ml}\left(t_{1,i},t_2\right)$ and $g_{ml}\left(t_{1,i},t_2\right)$.

The algorithm defined by (3.2)–(3.6) allows the simulator to evaluate the $\widehat{\boldsymbol{Y}}\left(t_{1,i},k\omega_p\right)$, for all $t_{1,i}=t_{1,1},t_{1,2},\ldots,t_{1,K_1}$, starting from a previously given initial condition $\widehat{\boldsymbol{Y}}\left(t_{1,0},k\omega_p\right)$. The way this initial condition is calculated will be described in Section 3.3.1.

3.3. Switching between numerical schemes

The newly proposed technique computes the solution of the circuit in the one-dimensional time t for the some time slots (here denoted as $[t_A,t_B]$) where SPICE is used, and in the bi-dimensional (t_1,t_2) framework for the remain time slots (here denoted as $[t_B,t_C]$) where the BHTF scheme is utilized. By performing the inverse Fourier transform of the solution computed with the BHTF scheme, we obtain the corresponding circuit bivariate solution $\widehat{y}(t_1,t_2)$ in the (t_1,t_2) framework. Thus, for the time slots in which the solution of the circuit is evaluated with SPICE, each of its state variables is a univariate entity. In contrast, for the time slots in which the solution of the circuit is evaluated with the BHTF scheme, each of its state variables is a bivariate function. Bivariate functions have then to be converted to their univariate forms according to (2.3). The flowchart depicted in Fig. 3.3 illustrates the global structure of the proposed switch mode simulation algorithm and its main steps. The most relevant mathematical details concerning the issues that have to be taken into account when performing transitions between different numerical schemes are provided in the following.

3.3.1. Switching from SPICE to BHTF

The SPICE engine is mainly used for the time slots where the stimulus is off (the "off-state" time slots), but not only there. Indeed, Fig. 3.1 illustrates that the SPICE stop point and the stimulus off–on transition time instant do not match. This means that the proposed method imposes a certain delay before the simulation engines are switched from SPICE to BHTF. The specific amount of this delay may differ from circuit to circuit, depending on its degree of complexity, the total number of dynamic elements, its time constants, and especially the discrepancy between the slowest and the fastest time scales. Therefore, automatically setting an appropriate value for this delay according to the circuit's stimuli, and the specifics of the circuit itself, is a crucial aspect. The automatic switching strategy proposed in this work is described as

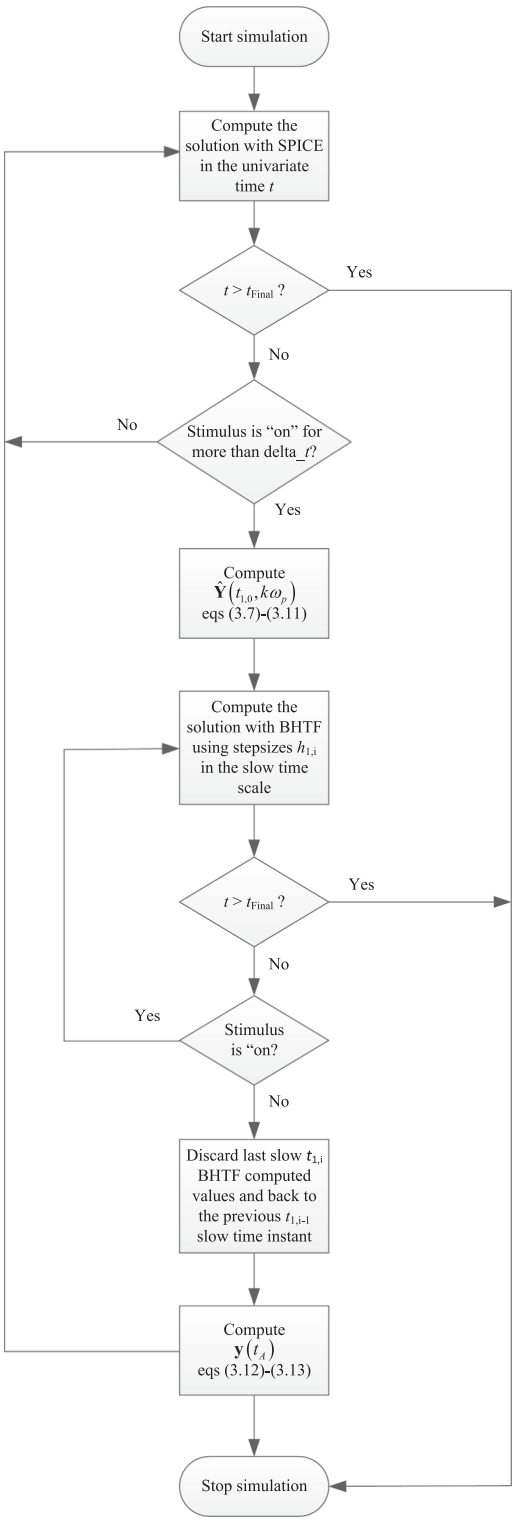

Fig. 3.3. Flowchart of the proposed simulation algorithm. Delta_t is a pre-defined delay, imposed by the simulator to provide BHTF acceptable starting values.

follows.

Let us define t_{ON} as the moment at which the simulator detects that the stimulus is turned on, i.e., the time instant from which $\|\boldsymbol{x}(t)\| > \delta$, where δ is a pre-defined small amount. The simulator initially starts by considering the instant $t_{ON} + h_1/2$. Then, the solution of the circuit is evaluated with the BHTF engine using one half of a slow stepsize, i.e., from $t_{ON} + h_1/2$ to $t_{ON} + h_1$, and also with the SPICE engine from t_{ON} to $t_{ON} + h_1$. The solutions obtained with BHTF and SPICE are then compared with each other within the interval $[t_{ON} + h_1/2,\ t_{ON} + h_1]$. If the solutions match (the discrepancy between solutions is below an allowed error ceiling), then the simulator switches to BHTF. If not, then the solution obtained with BHTF within the interval $[t_{ON} + h_1/2,\ t_{ON} + h_1]$ is discarded, and the simulator repeats the overall process for the next half slow stepsize.

A crucial aspect that must be taken into account when performing the transition from SPICE to BHTF is the evaluation of the initial condition $\widehat{\boldsymbol{Y}}(t_{1,0}, k\omega_p) \in \mathbb{C}^{N\times(2K+1)}$. This initial condition must be carefully computed from the numerical results previously obtained with SPICE for the simulation of the circuit during the first carrier cycles occurring immediately after the off–on transition time instant. The main aspects of the procedure adopted for computing $\widehat{\boldsymbol{Y}}(t_{1,0}, k\omega_p)$ are summarized in the following.

The proposed method starts by considering a time window comprising two consecutive carrier cycles around t_B, i.e., $[t_B - T_2, t_B + T_2]$, and the corresponding numerical univariate solution (numerical values evaluated with SPICE) on that time interval. These numerical univariate values will be mapped into the bidimensional $[t_B - T_2, t_B + T_2] \times [0, T_2]$ rectangular region according to (2.3), producing the following artificial bivariate vector-valued sets

$$\begin{aligned}&\boldsymbol{y}\widehat{(}t_B - T_2, 0) = \boldsymbol{y}(t_B - T_2)\widehat{\boldsymbol{y}}(t_B - T_2 + h, h) = \boldsymbol{y}(t_B - T_2 + h)\widehat{\boldsymbol{y}}(t_B - T_2 + 2h, 2h)\\ &= \boldsymbol{y}(t_B - T_2 + 2h)\,\vdots\,\widehat{\boldsymbol{y}}(t_B, t_B + T_2) = \boldsymbol{y}(t_B)\end{aligned} \tag{3.7}$$

and

$$\begin{aligned}&\widehat{\boldsymbol{y}}(t_B, 0) = \boldsymbol{y}(t_B)\widehat{\boldsymbol{y}}(t_B + h, h) = \boldsymbol{y}(t_B + h)\widehat{\boldsymbol{y}}(t_B + 2h, 2h)\\ &= \boldsymbol{y}(t_B + 2h)\,\vdots\,\widehat{\boldsymbol{y}}(t_B + T_2, T_2) = \boldsymbol{y}(t_B + T_2)\end{aligned} \tag{3.8}$$

These bivariate values will be then interpolated to generate another set of artificial bivariate values, denoted as $\widehat{\boldsymbol{y}}(t_B, t_{2,j})$, which can be seen as a set of N discrete artificial waveforms defined on the $(t_1 = t_B, 0 \leqslant t_2 \leqslant T_2)$ artificial time line. If time step size h is selected so that $M = T_2/h$ is an integer, and linear interpolation is used, $\widehat{\boldsymbol{y}}(t_B, t_{2,j})$ can be simply given by

$$\widehat{\boldsymbol{y}}(t_B, t_{2,j}) = \widehat{\boldsymbol{y}}(t_B + jh, jh) + jh\frac{\widehat{\boldsymbol{y}}(t_B - T_2 + jh, jh) - \widehat{\boldsymbol{y}}(t_B + jh, jh)}{T_2} j = 0, 1, 2, \ldots, M. \tag{3.9}$$

At this point the Fourier coefficients of each artificial waveform $\widehat{y}_v(t_B, t_{2,j})$, $v = 1, 2, \ldots, N$, will be evaluated by computing its discrete Fourier transform (DFT), given as

$$\widehat{\boldsymbol{Y}}_v(t_B, k\omega_p) = \sum_{j=0}^{M-1} \widehat{y}_v(t_B, t_{2,j}) \cdot e^{-ik\frac{2\pi}{M}j}, \quad v = 1, 2, \ldots, N, \tag{3.10}$$

in which M stands for the number of points of $\widehat{y}_v(t_B, t_{2,j})$ and i stands for the imaginary unit. Finally, since a convenient harmonic truncation at some order K was adopted in the BHTF scheme for the HB evaluations, it means that the circuit will not generate waveforms with harmonic

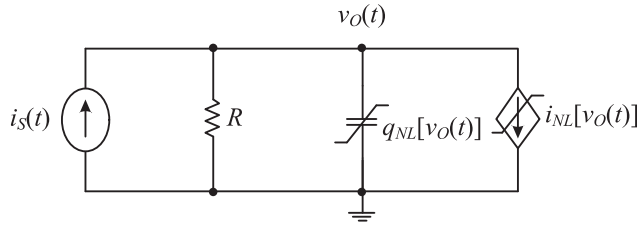

Fig. 4.1. Single node nonlinear dynamic circuit [29], composed of a current source connected to a linear resistance, a nonlinear capacitance and a nonlinear voltage-dependent current source.

components of order $k > K$. As a consequence, some of the $\widehat{\boldsymbol{Y}}_v(t_B, k\omega_p)$ Fourier coefficients will be null. Hence, each $\widehat{\boldsymbol{Y}}_v(t_{1,0}, k\omega_p)$ will be obtained from the corresponding $\widehat{\boldsymbol{Y}}_v(t_B, k\omega_p)$ by simply discarding its frequency components of order $k > K$. Finally, the starting condition $\widehat{\boldsymbol{Y}}(t_{1,0}, k\omega_p)$ necessary to compute the bivariate solution on the next $[t_B, t_C] \times [0, T_2]$ rectangular region will be given as

$$\widehat{\boldsymbol{Y}}t_{1,0}, k\omega_p) = \left[\widehat{\boldsymbol{Y}}_1(t_{1,0}, k\omega_p)^T, \widehat{\boldsymbol{Y}}_2(t_{1,0}, k\omega_p)^T, \ldots, \widehat{\boldsymbol{Y}}_N(t_{1,0}, k\omega_p)^T\right]^T \tag{3.11}$$

3.3.2. Switching from BHTF to SPICE

The bivariate hybrid time–frequency (BHTF) scheme is used for some specific portions of the time slots in which the stimulus is on (but not the entire "on-state" time slots). Fig. 3.1 illustrates that when an on–off transition occurs, there is anticipation before the simulation engines are switched from BHTF to SPICE. This is because the simulation process with BHTF is only viable if the circuit is excited by a stimulus containing a periodic component (e.g., an RF carrier). Since the h_1 slow time scale step size is, in general, much larger than the carrier period, when the stimulus is turned off at some time instant $t_{1,i}$ of the scheme defined by (3.1)–(3.6), the simulator has to go back to the previous slow time instant $t_{1,i-1}$ and stops using BHTF. At this point it will come again to the one-dimensional time t, to resume the evaluation of the solution with SPICE.

In summary, if the simulator detects that the stimulus is turned off for, at least, a small period (e.g. an half fast carrier cycle) before the time instant $t_{1,i}$, i.e., $\|\boldsymbol{x}(t)\| < \delta$ within the interval $[t_{1,i} - T_2/2, t_{1,i}]$, the solution computed with BHTF for the $[t_{1,i-1}, t_{1,i}] \times [0, T_2]$ bivariate rectangular region will be discarded. SPICE will be used to evaluate the solution from the $t_{1,i-1}$ time instant. With this strategy the simulator will be able to adapt itself again to the new circuit forcing function conditions, which will have significant impact in its transient response.

When jumping from the t_1, t_2 bidimensional space to the univariate time t the new lower limit t_A takes the value of $t_{1,i-1}$. This slow time instant $t_{1,i-1}$ will be considered as the old upper limit t_C for previous computations with BHTF in $[t_B, t_C] \times [0, T_2]$. The new initial condition, $\boldsymbol{y}(t_A)$, needed to evaluate the numerical solution of the circuit with SPICE in the following time window $[t_A, t_B]$ is obtained as

$$\boldsymbol{y}(t_A) = \left[\widehat{y}_1(t_C, 0), \widehat{y}_2(t_C, 0), \ldots, \widehat{y}_N(t_C, 0)\right]^T, \tag{3.12}$$

where each $\widehat{y}_v(t_C, 0)$ stands for the bivariate solution $\widehat{y}_v(t_C, t_{2,j})$ in the $(t_C, 0)$ grid point of the $[t_B, t_C] \times [0, T_2]$ rectangular region. Each $\widehat{y}_v(t_C, t_{2,j})$ is given by computing the inverse discrete Fourier transform of $\widehat{\boldsymbol{Y}}_v(t_C, k\omega_p)$. i.e.,

Table 1
Simulation of the circuit depicted in Fig. 4.1. Numerical results for simulations in the [0, 500 ns] interval using SPICE implementations based on the Gear–2 time-step integration scheme.

	CPU time (sec)			NMSE for the output voltage v_O	
Duty cycle	SPICE (Gear-2)	Method discussed in [12]	Proposed method	Method discussed in [12]	Proposed method
30%	57.92	50.14	46.32	5.32×10^{-7}	2.58×10^{-8}
50%	61.04	40.90	35.92	4.73×10^{-7}	1.62×10^{-8}
70%	63.72	34.72	26.64	4.15×10^{-7}	1.18×10^{-8}

Table 2
Simulation of the circuit depicted in Fig. 4.1. Numerical results for simulations in the [0, 500 ns] interval using SPICE implementations based on the Trapezoidal time-step integration scheme.

	CPU time (sec)			NMSE for the output voltage v_O	
Duty cycle	SPICE (Trapez.)	Method discussed in [12]	Proposed method	Method discussed in [12]	Proposed method
30%	53.21	47.52	43.01	6.26×10^{-7}	3.84×10^{-8}
50%	57.08	38.09	33.89	5.64×10^{-7}	2.17×10^{-8}
70%	58.85	32.48	24.77	4.98×10^{-7}	1.88×10^{-8}

Table 3
Simulation of the circuit depicted in Fig. 4.1. Numerical results for simulations in the [0, 500 ns] interval using SPICE implementations based on the Modified Trapezoidal time-step integration scheme.

	CPU time (sec)			NMSE for the output voltage v_O	
Duty cycle	SPICE (Modif. Trapez.)	Method discussed in [12]	Proposed method	Method discussed in [12]	Proposed method
30%	54.06	48.77	43.58	5.01×10^{-7}	2.44×10^{-8}
50%	57.27	38.95	34.02	4.55×10^{-7}	1.51×10^{-8}
70%	59.81	33.79	25.18	4.01×10^{-7}	1.09×10^{-8}

$$\widehat{y}_v(t_C, t_{2,j}) = \frac{1}{2K+1} \sum_{k=0}^{2K} \widehat{\boldsymbol{Y}}_v(t_C, k\omega_p)\, e^{ik\frac{2\pi}{2K+1}j}, \quad j = 0, \ldots, 2K, \quad v = 1, \ldots, N. \tag{3.13}$$

4. Illustrative application examples

In order to illustrate the capabilities of the method proposed in this paper, two application examples with distinct levels of complexity have been considered: (i) a single node nonlinear dynamic circuit and (ii) an on–off amplitude shift keying (OOK) wireless receiver. The numerical results presented in this section were all obtained with simulations conducted in MATLAB running on an Intel Core i7-2640 M CPU @ 2.80 GHz with 16 GB RAM computer.

4.1. Single node nonlinear circuit

The circuit depicted in Fig. 4.1 [29] was selected in view of the fact that, taking into account its very low complexity, it will be easy for any CAD researcher to replicate the numerical results here presented. This circuit is composed of a current source connected to a linear resistance, a nonlinear capacitance and a nonlinear voltage-dependent current source. The nonlinearities are described by the algebraic constitutive relations of voltage-dependent current and voltage-dependent charge defined in [29], with $I_0 = 0.4\,\text{mA}$, $\alpha = 1\,\text{V}^{-1}$ and $\tau_F = 2 \times 10^{-9}\text{s}$. The value $R = 1\,\text{k}\Omega$ was considered for the linear resistance of the circuit, and the current source $i_S(t)$ was considered as a fast RF carrier of 1 GHz fundamental frequency and 4.5 mA amplitude, being successively turned on and off at a rhythm of 20 million cycles per second, i.e., at every 50 ns.

The circuit was simulated in MATLAB with three different versions of the proposed switch mode simulation method (Gear–2 time-step integration combined with BHTF, trapezoidal time-step integration

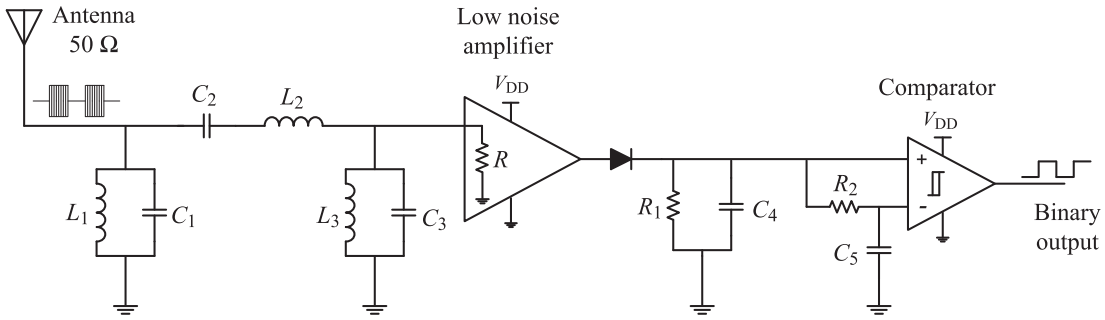

Fig. 4.2. Simplified schematic diagram of the simulated on–off amplitude shift keying wireless receiver.

Table 4
Simulation of the circuit depicted in Fig. 4.2. Numerical results for simulations in the [0, 10 μs] interval using SPICE implementations based on the Gear–2 time-step integration scheme.

	CPU time (h:min:sec)			NMSE 1		NMSE 2	
Duty cycle	SPICE (Gear-2)	Method discussed in [12]	Proposed method	Method discussed in [12]	Proposed method	Method discussed in [12]	Proposed method
30%	01:35:18	01:15:19	01:11:14	5.74×10^{-6}	9.02×10^{-7}	3.65×10^{-6}	6.46×10^{-7}
50%	01:45:20	01:05:46	00:57:02	5.31×10^{-6}	8.30×10^{-7}	3.36×10^{-6}	6.07×10^{-7}
70%	01:52:50	00:55:36	00:37:22	4.97×10^{-6}	7.45×10^{-7}	3.01×10^{-6}	5.54×10^{-7}

Table 5
Simulation of the circuit depicted in Fig. 4.2. Numerical results for simulations in the [0, 10 μs] interval using SPICE implementations based on the Trapezoidal time-step integration scheme.

	CPU time (h:min:sec)			NMSE 1		NMSE 2	
Duty cycle	SPICE (Trapez.)	Method discussed in [12]	Proposed method	Method discussed in [12]	Proposed method	Method discussed in [12]	Proposed method
30%	01:31:38	01:13:31	01:08:42	6.11×10^{-6}	9.91×10^{-7}	3.87×10^{-6}	6.81×10^{-7}
50%	01:41:14	01:02:40	00:55:04	5.77×10^{-6}	9.22×10^{-7}	3.52×10^{-6}	6.39×10^{-7}
70%	01:49:27	00:52:04	00:36:30	5.24×10^{-6}	8.26×10^{-7}	3.20×10^{-6}	5.97×10^{-7}

Table 6
Simulation of the circuit depicted in Fig. 4.2. Numerical results for simulations in the [0, 10 μs] interval using SPICE implementations based on the Modified Trapezoidal time-step integration scheme.

	CPU time (h:min:sec)			NMSE 1		NMSE 2	
Duty cycle	SPICE (Modif. Trapez.)	Method discussed in [12]	Proposed method	Method discussed in [12]	Proposed method	Method discussed in [12]	Proposed method
30%	01:31:59	01:13:54	01:08:54	5.46×10^{-6}	8.64×10^{-7}	3.52×10^{-6}	6.28×10^{-7}
50%	01:41:50	01:02:59	00:55:44	5.18×10^{-6}	7.93×10^{-7}	3.24×10^{-6}	5.88×10^{-7}
70%	01:49:53	00:52:46	00:36:47	5.05×10^{-6}	7.04×10^{-7}	2.92×10^{-6}	5.32×10^{-7}

combined with BHTF and modified trapezoidal time-step integration combined with BHTF) against: (i) the corresponding conventional time-step integration (SPICE) algorithm and (ii) the simulation technique discussed in [12]. The reasons for these comparisons are: (i) SPICE is the numerical technique used by commercial and free packages for simulating a circuit having this kind of intermittent stimulus. Other well established techniques, like steady-state engines [30] or envelope following schemes, assume that the circuits are uninterruptedly forced by stimuli containing a periodic component (an RF carrier, an envelope modulated signal, etc.) which is not the case discussed in this paper; (ii) the time slot partition technique previously published in [12] is suitable to deal with this kind of circuits, but cannot compute smooth narrow-band RF modulated signals in the frequency domain.

Numerical results for simulations in the $[0,\ 500\ \text{ns}]$ interval are presented in Tables 1–3. A time-step integration size $h = 10$ ps (100 steps per RF carrier cycle) was used in the univariate time scale t, whereas $h_1 = 10$ ns was chosen for the slow time scale t_1. $K = 12$ was considered as the maximum harmonic order for the HB evaluations. The percentage of time in which the RF carrier is active compared to its on–off switching period (duty cycle) was manually modified to determine the influence of this parameter on the efficiency of the method. As expected, speedup increases with duty cycle. The reason for that is because time intervals in which the solution of the circuit has to be computed with SPICE become smaller.

Tables 1–3 also present some normalized mean square error (NMSE) values for the $v_O(t)$ voltage. The NMSE parameter (here considered as the accuracy criterion) estimates the overall deviations between the solution obtained with the proposed method, as well as the method discussed in [12], when compared to the solution computed with the standard time-step integration engine. As can be seen, the accuracy of the results obtained with the proposed method is very good.

Finally, numerical results summarized in Tables 1–3 evidence that gains in computation speed obtained with the new proposed method are reasonably independent of the SPICE implementation code. They also evidence a slight improvement in terms of both accuracy and computational effort in comparison to the method discussed in [12].

Table 7
Simulation of the circuit depicted in Fig. 4.2. Numerical results for simulations in the [0, 10 μs] interval using SPICE implementations based on a Runge-Kutta (RK) time-step integration scheme.

	CPU time (h:min:sec)			NMSE 1		NMSE 2	
Duty cycle	SPICE (RK)	Method discussed in [12]	Proposed method	Method discussed in [12]	Proposed method	Method discussed in [12]	Proposed method
30%	01:41:45	01:19:24	01:16:52	8.29×10^{-6}	1.02×10^{-6}	4.30×10^{-6}	7.32×10^{-7}
50%	01:49:21	01:08:31	01:01:24	7.01×10^{-6}	9.95×10^{-7}	3.84×10^{-6}	6.61×10^{-7}
70%	01:59:33	00:58:50	00:39:52	6.15×10^{-6}	8.85×10^{-7}	3.30×10^{-6}	6.05×10^{-7}

Table 8
Simulation of the circuit depicted in Fig. 4.2. Numerical results for simulations in the [0, 10 μs] interval using SPICE implementations based on a Multirate Runge-Kutta (MRK) time-step integration scheme.

	CPU time (h:min:sec)			NMSE 1		NMSE 2	
Duty cycle	SPICE (MRK.)	Method discussed in [12]	Proposed method	Method discussed in [12]	Proposed method	Method discussed in [12]	Proposed method
30%	01:44:33	01:21:50	01:20:41	8.48×10^{-6}	1.12×10^{-6}	4.41×10^{-6}	7.29×10^{-7}
50%	01:52:42	01:11:00	01:04:55	7.20×10^{-6}	9.74×10^{-7}	3.90×10^{-6}	6.84×10^{-7}
70%	02:03:56	01:02:46	00:42:30	6.13×10^{-6}	8.90×10^{-7}	3.34×10^{-6}	6.10×10^{-7}

4.2. OOK wireless receiver

In order to test the capabilities of the proposed simulation algorithm in a real world example of practical interest the circuit illustrated in Fig. 4.2 will be now considered. The circuit depicted in Fig. 4.2 is a simplified schematic of an on–off amplitude shift keying (OOK) wireless receiver. This circuit comprises four blocks: (i) an input band-pass filter to discern the carrier frequency of interest (450 MHz) from a broadband input spectrum; (ii) a low noise amplifier (LNA); (iii) an envelope detector to extract the information of interest and (iv) a high-speed comparator to obtain the binary outputs. The comparator trigger threshold is obtained from the output of the envelope detector itself, enabling the threshold level to auto-scale with the received signal level. The values of the passive components of the circuit are: $C_1 = 31.83$ pF, $L_1 = 3.93$ nH, $C_2 = 0.786$ pF, $L_2 = 159.16$ nH, $C_3 = 31.83$ pF, $L_3 = 3.93$ nH, $R = 50\ \Omega$, $R_1 = 100$ kΩ, $C_4 = 0.2$ pF, $R_2 = 1$ MΩ, $C_5 = 2$ pF. Since the circuit was designed for a 2 Mbps data rate, the baseband digital data was here considered as a rectangular wave of 1 MHz fundamental frequency modulating a high frequency carrier of 450 MHz. Thus, the stimulus can be seen as a 450 MHz sinusoidal source being successively turned on and off at a rhythm of 1 million times per second.

As in the previous example, we first simulated the circuit in MATLAB with three different versions of the proposed method (combining three distinct LMM with BHTF) against: (i) the corresponding conventional time-step integration (SPICE) algorithm and (ii) the simulation technique discussed in [12]. Numerical simulation results for simulations in the $[0,\ 10\ \mu s]$ interval are presented in Tables 4–6. A dynamic step length h and $h_1 = 100$ ns were chosen for the univariate and slow time scales, respectively. $K = 20$ was considered as the maximum harmonic order for the HB evaluations. Once again, with the intention of measuring the influence of the "on" and "off" states' duration in the efficiency of the method, the baseband digital data was considered as a rectangular wave of adjustable duty cycle.

In the same way as in the previous application example, the analysis of the results presented in Tables 4–6 can attest the improvements brought by the proposed method. A significant speedup raise is observed when the input duty cycle is increased, i.e., when the number of '1' symbols is higher than the number of '0' symbols. Although we might think that in practical OOK transceivers the '1' and '0' symbols tend to be equally probable, this does not necessarily mean that the duration of the "on" and "off" states tends to be the same. For instance, in RFID applications, in which pulse-interval encoding (PIE) is commonly used, a binary '1' is coded as a short power-off pulse following a long full-power interval (duty cycle > 50%), and a binary '0' is coded as a shorter full-power interval with the same power-off pulse (duty cycle = 50%). However, Tables 4–6 show that even in the situation of an average duty cycle of 50% the proposed method is more efficient than the traditional SPICE.

Once again, with the intention of providing a general idea for the accuracy of the results obtained with the proposed method two NMSE values are presented in Tables 4–6. NMSE 1 represents the highest of all NMSE values of the circuit state variables (voltages and currents). NMSE 2 represents the mean of these NMSE values. As can be observed, the accuracy of the results is very satisfactory.

As stated above, conventional time-domain circuit simulation is commonly achieved through the employment of linear multistep second order backward-differentiation-formulas. Indeed, few attempts have been made for applying Runge Kutta schemes to the analysis of electronic circuits in commercial simulators. Despite this fact, and with the intention of providing a more general study in this work, the circuit of Fig. 4.2 was also simulated in MATLAB with two new different versions of the proposed switch mode simulation algorithm, combining now RK and MRK formulas with BHTF. The results of these simulations are summarized in Tables 7 and 8.

Numerical results shown in Tables 4–8 evidence that gains in computation speed obtained with the new proposed method are practically independent of the SPICE implementation code. They also evidence a noteworthy improvement in comparison to the method discussed in [12]. The main reason for that is because the approach previously advanced in [12] (which was also conceived to deal with circuits containing stimuli being successively turned on and off for unknown periods of time) is a purely time-domain technique, in which the simulation algorithm is automatically switched between a SPICE engine and an envelope transient over shooting scheme. Thus, the technique proposed in [12] is not able to take advantage of the circuits' moderate nonlinearities, and their corresponding smooth narrowband RF modulated signals, which can be more efficiently computed in the frequency domain than in time domain.

It is also worth to highlight that the use of the MRK scheme (Table 8) has not led to any computational savings, in comparison to LMM or RK versions (Tables 4–7). The reason for that is because the multirate behavior exhibited by the kind circuits under analysis (circuits driven by fast stimuli being successively turned on and off) does not concern to the coexistence of fast and slow state variables in the same problem. Actually, as seen above, this multirate behavior relies on fast signals containing parameters that evolve themselves at separated time scales.

As a final remark, it must be added that several other simulations of the circuit, under different conditions and different time intervals, have been conducted and the results obtained were always similar to the ones presented in Tables 4–8.

5. Conclusions

In this paper an innovative switch mode simulation algorithm was discussed and tested. The proposed method is based on a time-slot partitioning technique, with automatic switching between univariate time-step integration schemes and bivariate hybrid time–frequency engines, and is particularly suitable for computing the solution of RF circuits whose stimuli are continuously turned on and off for unknown periods of time. The method enables significant reductions on the computational effort, when compared to conventional time-step integration engines (the unique simulation engines available in commercial CAD tools that are able to simulate this kind of circuits), without losing the accuracy. By operating in both time and frequency domains the proposed method also circumvents some limitations of previously published work.

Although the efficiency of the method here discussed is already quite significant for the tested illustrative examples, it has been demonstrated that this efficiency will be made more and more evident for circuits in which the duration of the "on-state" periods is longer than their "off-state" time intervals.

Finally, it is worth to point out that, although the scope of this paper is essentially devoted to the RF simulation field, the proposed method can also be used to compute the numerical solution of generic electronic systems containing periodic forcing functions being successively switched on and off. Hence, in addition to the RF/microwave engineering community, this paper can also be of great interest to any researcher working in CAD techniques for nonlinear analysis and system simulation.

Declaration of Competing Interest

The authors declare that they have no known competing financial interests or personal relationships that could have appeared to influence the work reported in this paper.

Acknowledgments

This work is funded by National Funds through FCT – Fundação para a Ciência e Tecnologia, under the project UIDB/50008/2020-UIDP/50008/2020.

References

[1] Kabir M, Christoffersen C, Kriplani N. Transient simulation based on state variables and waves. Int J RF Microwave Comput Aided Eng 2011;21(3):314–24.
[2] Oliveira JF. Radio frequency and microwave numerical simulation techniques based on multivariate formulations. Appl Math Comput 2017;294:238–52.
[3] Bittner K, Brachtendorf HG. Multi-rate coupled circuit-device simulation. In: Proc. 26th International Conference Radioelektronika, Kosice; 2016, p. 42–7.
[4] Oliveira JF, Pedro JC. A new mixed time-frequency simulation method for nonlinear heterogeneous multirate RF circuits. In: Proceedings of the IEEE MTT-S International Microwave Symp. Digest, Anaheim CA; May 2010, p. 548–51.
[5] Oliveira JF, Pedro JC. Efficient RF circuit simulation using an innovative mixed time-frequency method. IEEE Trans Microw Theory Tech 2011;59(4):827–36.
[6] Brazil TJ. Time-domain techniques in microwave circuit simulation. IET Microwaves Antennas Propag 2013;7(2):146–55.
[7] Farhan MA, Gad E, Nakhla MS, Achar R. Fast simulation of microwave circuits with nonlinear terminations using high-order stable methods. IEEE Trans Microw Theory Tech 2013;61(1):360–71.
[8] Bizzarri F, Brambilla A, Codecasa L. Harmonic balance based on two-step Galerkin method. IEEE Trans Circ Syst I Regul Pap 2016;63(9):1476–86.
[9] Carvalho NB, Pedro JC, Jang W, Steer MB. Nonlinear RF circuits and systems simulation when driven by several modulated signals. IEEE Trans Microw Theory Tech 2006;54(2):572–9.
[10] Rizzoli V, et al., Domain-decomposition harmonic balance with block-wise constant spectrum. In: Proc. IEEE MTT-S Int. Microwave Symp. Digest, San Francisco, CA; Jun. 2006, p. 860–3.
[11] Oliveira JF, Pedro JC. A multiple-line double multirate shooting technique for the simulation of heterogeneous RF circuits. IEEE Trans Microw Theory Tech 2009;57(2):421–9.
[12] Ferreira D, Oliveira JF, Pedro JC. A novel time-domain CAD technique based on automatic time-slot division for the numerical simulation of highly nonlinear RF circuits. IEEE Trans Microw Theory Tech 2014;62(1):18–27.
[13] Bittner K, Brachtendorf HG. Adaptive multi-rate wavelet method for circuit simulation. Radioengineering 2014;23(1):300–7.
[14] Hsieh J, Huang Y, Kuo P, Wang T, Lu S. A 0.45-V Low-Power OOK/FSK RF receiver in 0.18μm CMOS technology for implantable medical applications. IEEE Trans Circ Syst I Regul Pap 2016;63(8):1123–30.
[15] Kim SJ, Park CS, Lee S. A 2.4-GHz ternary sequence spread spectrum OOK transceiver for reliable and ultra-low power sensor network applications. IEEE Trans Circ Syst I Regul Pap 2017;64(11):2976–87.
[16] Hien-Hua Jung, Kea-Tiong Tang. A 0.9-V 2.36-GHz MedRadio-band 10-Mbps low-power OOK modulator for neural implants. In: 2017 International Symposium on VLSI Design, Automation and Test (VLSI-DAT), Hsinchu; 2017, p. 1–4.
[17] Zhu H, Goi K, Ogawa K. All-Silicon waveguide photodetection for low-bias power monitoring and 20-km 28-Gb/s NRZ-OOK signal transmission. IEEE J Sel Top Quantum Electron 2018;24(2):1–7.
[18] Pires SC, Cabral PM, Pedro JC. Radio frequency carrier amplitude-burst transmitters - from architecture to circuit. IET Microwaves Antennas Propag 2015;9(3):271–80.
[19] Song Y, Zhu R, Wang YE. An X-Band pulsed load modulation transmitter with multilevel envelope delta–sigma modulations. IEEE Trans Microw Theory Tech 2016;64(11):3643–53.
[20] Jouzdani M, Ebrahimi MM, Helaoui M, Ghannouchi FM. Complex delta–sigma-based transmitter with enhanced linearity performance using pulsed load modulation power amplifier. IEEE Trans Microw Theory Tech 2017;65(9):3324–35.
[21] Sharrit D. Method for simulating a circuit. U.S. Patent 5588142, December 24; 1996.
[22] Ngoya E, Larchevèque R. Envelope transient analysis: a new method for the transient and steady-state analysis of microwave communications circuits and systems. In: Proceedings if the IEEE MTT-S International Microwave Symposium Digest, San Francisco CA; 1996, p. 1365–8.
[23] Hairer E, Nørsett S, Wanner G. Solving ordinary differential equations I: nonstiff problems. Berlin: Springer-Verlag; 1987.
[24] Hairer E, Wanner G. Solving ordinary differential equations II: stiff and differential algebraic problems. Berlin: Springer-Verlag; 1991.
[25] Brachtendorf H, Welsch G, Laur R, Bunse-Gerstner A. Numerical steady-state analysis of electronic circuits driven by multi-tone signals. Electric Eng (Springer-Velag) 1996;79(2):103–12.
[26] Mei T, Roychowdhury J, Coffey T, Hutchinson S, Day D. Robust stable time-domain methods for solving MPDEs of fast/slow systems. IEEE Trans Comput Aided Des Integr Circuits Syst 2005;24(2):226–39.
[27] Rodrigues PJ. Computer-aided analysis of nonlinear microwave circuits. Norwood, MA: Artech House; 1998.
[28] Maas SA. Nonlinear microwave and RF circuits. 2nd ed. Norwood, MA: Artech House; 2003.
[29] Pedro JC, Carvalho NB. Intermodulation distortion in microwave and wireless circuits. Norwood: Artech House; 2003.
[30] Kundert K, White J, Sangiovanni-Vincentelli A. Steady-state methods for simulating analog and microwave circuits. Norwell, MA: Kluwer Academic Publishers; 1990.